Journal of Natural Gas Science and Engineering 76 (2020) 103181

Contents lists available at ScienceDirect

Journal of Natural Gas Science and Engineering

journal homepage: http://www.elsevier.com/locate/jngse

Coalbed methane reservoir fracture evaluation through the novel passive microseismic survey and its implications on permeable and gas production

Lin Tian [a,b], Yunxing Cao [a,b,c,d,*], Shimin Liu [c,e], Bin Shi [a,b], Jianzhong Liu [f], Derek Elsworth [e]

[a] School of Resources and Environment, Henan Polytechnic University, Jiaozuo 454000, China
[b] Research Center of Coalbed Methane/Gas Geology and Engineering, Henan Polytechnic University, Jiaozuo 454000, China
[c] Henan International Joint Laboratory for Unconventional Energy Geology and Development, Henan Polytechnic University, Jiaozuo 454000, China
[d] Henan Provincial Collaborative Innovation Center of Coalbed Methane and Shale Gas for Central Plains Economic Region, Henan Polytechnic University, Jiaozuo 454000, China
[e] Department of Energy and Mineral Engineering, G^3 Center and Energy Institute, Pennsylvania State University, University Park, PA 16802, USA
[f] Beijing Traverse Technology and Development Company Limited, Beijing 100100, China

ARTICLE INFO

Keywords:
CBM
Fractures
Microseismic survey
Focal mechanism
Gas production

ABSTRACT

Fracture networks in coalbed reservoirs serve as the primary gas pathway and thus determine the gas production potential for coalbed methane (CBM) recovery. However, the characterization of the fracture network is extremely challenging due to the complexity of both the induced and natural fracture system. A microseismic event analysis can be used to locate the fracturing, and determine the orientation, length, complexity, and temporal growth of the induced fracture by using the focal mechanism. In this study, the fracture system of a coal-bearing formation covering 1.2 km^2 in the Luan mining area of China is probed via passive microseismic imaging. Focal mechanisms of individual events are used to characterize the gas production potential for the 10 CBM wells in this area. Fracture reactivation modes are of three types - strike slip, dip slip, and extensional modes – with strike slip the most common followed by dip slip and then extensional type as the least likely. In addition, the location of different types of fractures are different, which indicates the difference of the in-situ stress regime. The 10 CBM wells were hydraulically stimulated in December 2017 then dewatered and allowed to produce for 14 months. We show that the microseismic data have a general positive correlation with gas production with a few exceptions - the higher the event count, the higher the gas production. This result is a best embodiment of the mutual control of reservoir fractures, stress regime, permeable and gas production in CBM development. We suggest passive microseismic imaging as an effective technique in evaluating the potential for gas production.

1. Introduction

The presence of methane in high concentrations and at high pressures is a root cause for gas outbursts and explosions in coal mines – an adverse effect that can be mitigated by drainage. Twenty-five catastrophic coal mine accidents with more than 100 fatalities have occurred over the last seven decades in China and the presence of excess methane has been implicated in 18 out of these 25 catastrophic coal mine disasters (Yu, 2007). Coal mine methane remains the single greatest hazard in incidents and/or disasters. Thus, the extraction of methane, either in-mine or from surface boreholes is the top priority for mine safety control for underground coal mines in China (National energy administration, 2005; Liao et al., 2012; Research center of oil, 2009). Coalbed methane (CBM) extraction from surface wellbores provides an additional energy resource in which the natural gas is utilized and additionally reduces the carbon footprint by burning CBM rather than coal. In China, the mine operators are the main proponents for CBM extraction to the surface – as this not only shortens the gas drainage period prior to the recovery of the main resource (coal), but also adds revenue from both the sale of gas and in receiving tax incentives from federal and local governments (Palmer, 2010; National energy board 2007; Ece energy series 2010; Mu, 2017; Cao et al., 2014; Men et al., 2017).

However, the CBM industry in China has grown only incrementally over the last two decades due to the low permeability of the coal seams and the complex geological conditions. In 2017, 17,496 CBM wells were active and producing, but the annual production was only 4.9 billion m^3 (Men et al., 2018). Underperforming CBM wells are very common across

* Corresponding author. School of Resources and Environment, Henan Polytechnic University, Jiaozuo 454000, China.
E-mail address: yxcao17@126.com (Y. Cao).

https://doi.org/10.1016/j.jngse.2020.103181
Received 30 July 2019; Received in revised form 18 January 2020; Accepted 18 January 2020
Available online 22 January 2020
1875-5100/

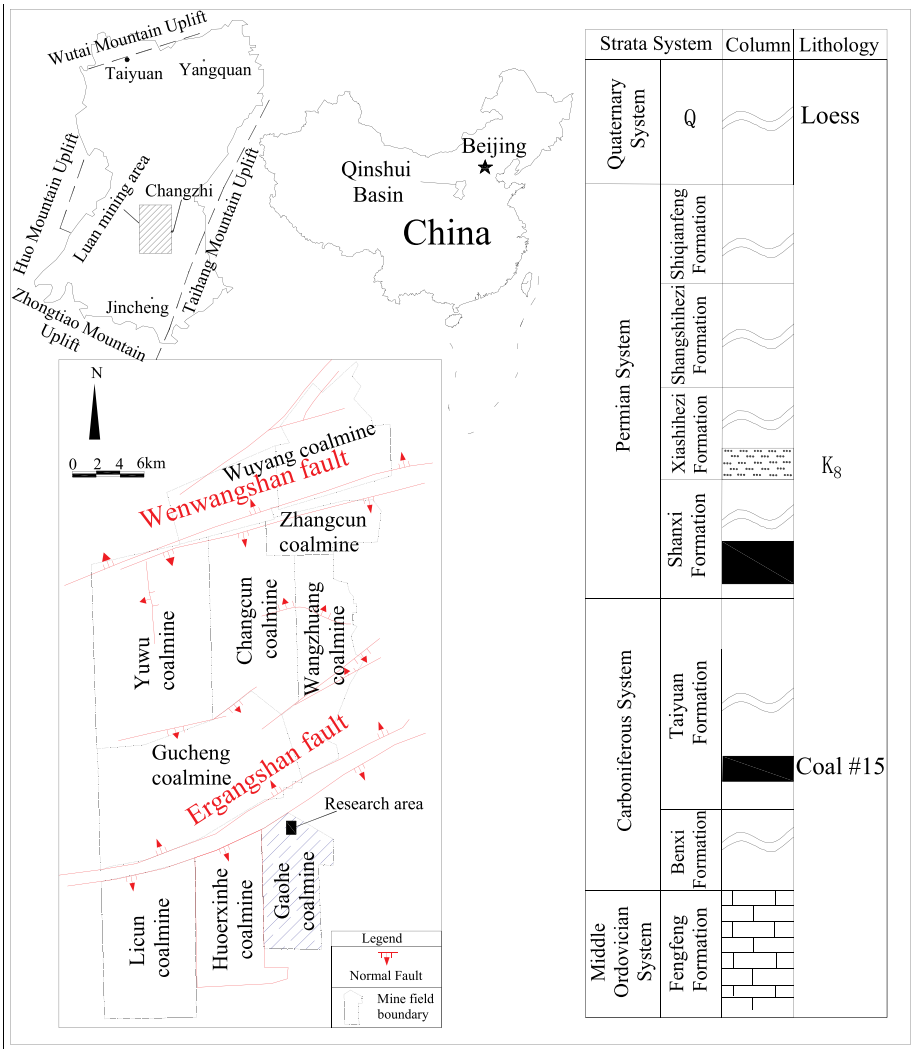

Fig. 1. Geological setting of the Luan area together with the stratigraphic column (Tian et al., 2015).

the entire nation. CBM production may be significantly increased if regions with high native permeability and simple geological structures can be identified. Alternatively, improved drilling and stimulation technologies may be applied to existing low permeability and complex formations to achieve this goal. Indeed, these activities are closely interrelated as effective methods to both identify areas of high native permeability, and to further increase this permeability by stimulation offer additive improvements. To this goal, there are many technologies to identify in situ permeability and gas rate potential. Dominant methods include injection fall-off tests (IFOT) and drill rig tests (DST) to define in situ reservoir permeability either during the drilling period or before stimulation (Rodvelt and Oestreich, 2008). These are expensive methods for obtaining permeability for targeted formations and in highly anisotropic and heterogeneous reservoirs they only return an average volumetric and non-directional permeability. A second alternative in characterizing the permeability of a CBM play is to apply structural-geology-based methods including structural curvature and fracture system analysis (Davis et al., 2011; Groshong et al., 2009). A structural curvature index is estimated based on the details of folding within the geological system, including both anticlines and synclines of a coalbed or a coal bearing formation. Usually, a 3D seismic survey map is required to reliably define structure. In a newly developed CBM block with little structural data, the curvature index is typically poorly defined and must be carefully constrained.

Fracture (and/or joint) system analysis is a third method broadly applied to define structure or stress regime in reservoirs (Dixon, 1979; Wheeler and Dixon, 1980). Fracture data, including attitude, orientation, aperture, spacing or density are interpreted from surface outcrops of the formation through field investigation. Similar correlations between the coal cleat systems and permeability are broadly utilized in the description of CBM geology (Chen et al., 2018; Liu, 2013). Fracture analysis results describe the stress regime and its geological evolution, fracture density distribution, and frequency. It can also serve as a proxy for permeability and production potential of the corresponding CBM reservoir. Coal seams with denser networks of fractures evident in surface outcrops typically have well connected fracture/cleat system with relatively high permeability and thus have better production potential, and vice versa (Pashin and Groshong, 1998; Bo et al., 2008; Laubach et al., 1998). Thus, the fracture system significantly influences reservoir permeability and its evolution with gas production which determines the gas production profile. This phenomenon has been confirmed in the Qinshui basin and Xinjiang Fukang mining areas (Zhang, 2016). However, in many CBM plays and coal mining areas, thick coverings of Quaternary loess and an absence of outcrops restrict or eliminate the potential of fracture investigation through structural investigation. Thus, the development of a new straightforward method to reliably evaluate permeability and potential gas production from CBM reservoirs is important for the future evaluation of CBM production and resource quantification.

In recent years, using microseismic monitoring data to improve yield

has become a common method for deep engineering such as shale gas production, petroleum hydraulic fracturing, and geothermal development. Microseismic monitoring is a potentially useful approach for capturing the space-time distribution of fractures and fluid migration in rock masses (Maxwell et al., 2010; Detring and Williams-Stroud, 2012; Lacazette and Laudon, 2015; Zhao et al., 2019). However, studies on the microseismic monitoring are less common in reservoir characterization than in the evaluation of hydraulic fracturing performance. The aim of this study is to propose a microseismic method for fracture characterization of deep coal seams. In addition, the linkage of reservoir properties impacting permeability and gas production is studied. Finally, taking the Luan mining area as a case study, the evaluation of gas production potential using passive microseismic monitoring was verified by the production data from 10 wells.

2. Geological setting and reservoir properties

2.1. Regional geology

The study area, the Luan mining area, is in the southeastern limb of the Qinshui basin (Fig. 1), Shanxi province. This mining area covers approximately 3,464 km^2 with CBM resources estimated to be 334.7 billion m^3, and is one of the largest CBM plays in China (Tian et al., 2015). The Qinshui basin is known to be a great complex syncline covering an area of 29,000 km^2–36,000 km^2, where the coal mining industry and CBM wells were extensively developed since the last century. The basin tectonically formed during the Mesozoic Era and is surrounded by four uplifts: the Taihang Mountain to the east, the Lvliang Mountain to the west, the Wutai Mountain to the north and the Huo and Zhongtiao Mountains to the southwest. Following uplift and erosion, the Qinshui basin evolved as a complex syncline striking NNE-SSW in North China. In the Luan mining area, strata strike north-south and dip to the west at an angle of 5°–10°, and a group of faults and smaller folds were observed during the coal and CBM mining period. These folds consist of parallel anticlines and synclines, with the majority striking north-south (Cai et al., 2011).

The major fault systems in the study area are complex. As shown in Fig. 1, the Wenwangshan normal fault in the north, and the Ergangshan normal faults in the south separate the mining area into three blocks. The two major faults consist of two parallel normal faults respectively (Tian et al., 2015). The research area of the Gaohe coal mine is in the southeastern extent of the Luan mining area.

2.2. Stratigraphy and coal bearing formations

In the study area, the Carboniferous and Permian are the strata bearing coal and CBM. The Carboniferous strata consists of the Benxi and Taiyuan Formations, and the Permian strata consists of the Shanxi, Xiashihezi, Shangshihezi, and Shiqianfeng Formations (Fig. 1). The Taiyuan and Shanxi Formation are two major coal bearing formations, and they were estimated to have a combined mean thickness of ~150 m. Coal #15 in the Taiyuan Formation has a mean thickness of 4 m. The coal #3 in the Shanxi Formation with a mean thickness of ~6 m is the most continuous and stable mining and CBM target seam in this study area. The current burial depth of coal #3 varies from 400 m in the east to 1200 m in the west. With increasing burial depth, coal #3 increases in gas content, and in rank from lean coal to anthracite, while the vitrinite reflectance ($R_{o,\ max}$) increases from 2.0% to 2.5% (Tian et al., 2015; Cai et al., 2011).

2.3. Local microseismic survey

The study area contains eight large coal mines operated by the Shanxi Luan Coal Mining Group (Fig. 1). The study area extends over 1.2 km^2 and is in the north of the Gaohe coal mine in the south-eastern extent of the mining area. Ten surface CBM wells were drilled and completed in the area in 2012. This limited area comprises a monoclinic structure dipping to the west with a group of secondary synclines and anticlines as shown in Fig. 2.

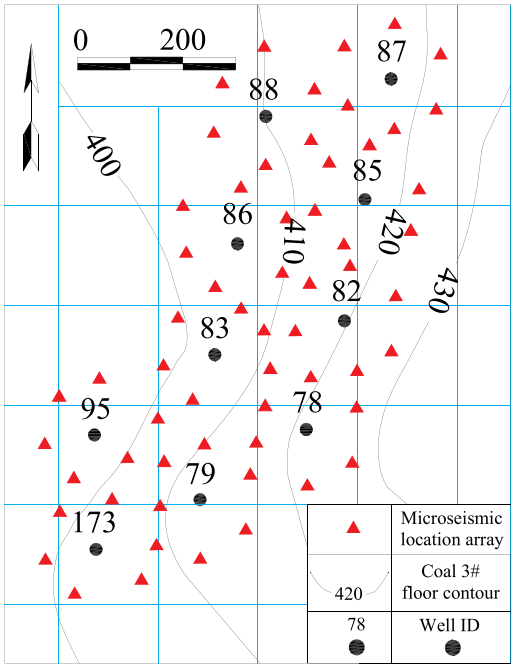

Fig. 2. Well location and structural map of the research area.

Table 1
Coal parameters in the #3 reservoir.

Well ID	Depth/m	H/m	T/m	P (MPa)	P_{cd} (MPa)	K (mD)
HG78	493.2	422.09	6.25	2.42	1.06	
HG79	507.3	415.82	7.1	2.24	1.02	
HG82	504.85	422.25	5.3	2.48	1.53	0.45
HG83	524.74	401.86	6	2.79	1.05	
HG85	512.95	414.77	7.8	2.63	1.2	
HG86	522.68	405.15	6.65	2.88	0.87	
HG87	512.17	415.87	7.1	2.17	0.96	
HG88	517.57	410.32	7.1	2.26	0.78	0.058
HG95	531.87	393.75	7.1	2.62	0.86	0.083
HG173	512.6	402.85	6.6	1.62	0.62	

Where: H is the floor elevation of the #3 coal seam; T is the thickness of the seam; P is the reservoir pressure, P_{cd} is the critical desorption pressure, and K is the reservoir permeability recovered form injection fall-off tests.

The land surface of the study area is gently rolling and covered with Quaternary loess approximately 150 m thick. Table 1 lists the detailed coal and reservoir properties of the #3 coal seam. The occurrence of the #3 seam is stable with thickness varying from 5.3 m to 7.8 m. The current burial depth of the coal varies between 493.2 m and 531.8 m, with an average of 513.9 m. The reservoir pressure varies from 1.62 MPa to 2.88 MPa, with permeability recovered from injection falloff tests in 3 wells in the range 0.058 mD to 0.45 mD.

3. Methodology

3.1. Microseismic monitoring and focal mechanisms

Microseismic monitoring has proven to be a valuable method for monitoring the propagation of hydraulic fractures, and in determining other reservoir properties. This includes the potential to provide estimates of important reservoir characteristics including natural fracture orientations, stress fields and other information about the hydraulic fracturing process (Jupe et al., 1998; Li et al., 2019; Eyre and van der

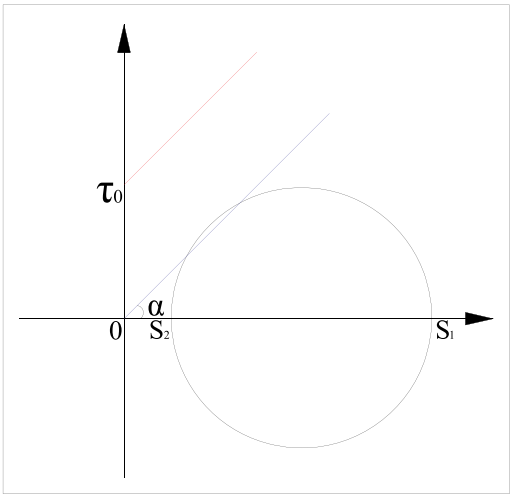

Fig. 3. Mohr circle of stress. Where, S_1 is the maximum principal stress, S_2 is the minimum principal stress, and τ_0 is the cohesion of intact rock. The red line and blue lines represent the envelope for primary fractures with and without rock cohesion respectively.

Baan, 2015; Zhao et al., 2019).

CBM reservoirs have undergone coalification, and tectonic deformation typically develops a complex fracture system. Seismic events represent stress release and typically occur along pre-existing fractures rather than in areas of previously unbroken rock (Combs and Hadley, 1977). Further, excellent correlation exists between zones of rupture and mapped faults where earthquakes have been located in sufficient number to define a pattern (Combs and Hadley, 1977; Malin et al., 1989).

Relative shear slip displacement in the subsurface is the primary source of microseismic events. The basic model for passive microseismic monitoring relates to the Mohr-Coulomb criterion and the estimated Coulomb shear stress on the sliding surface is given as:

$$\tau \geq \tau_0 + \frac{\mu(S_1 + S_2 - 2P_0)}{2} - \frac{\mu(S_1 - S_2)}{2}\cos(2\alpha) \quad (1)$$

and

$$\tau = \frac{S_1 - S_2}{2}\sin(2\alpha)\ , \quad (2)$$

where, τ (MPa) is the shear stress on the sliding surface; τ_0 (MPa) is the shear strength of the rock independent of directional stress (cohesion); S_1 and S_2 (MPa) are the maximum and minimum horizontal principal stresses respectively; P_0 (MPa) is the pore pressure; μ is the internal friction coefficient of rock; and α (°) is the included angle between the maximum principal stress and sliding surface along the sliding direction.

An increase in the maximum principal stress S_1, a decrease in the minimum principal stress S_2, an increase in the pore pressure P_0, or a change in the orientation of the slip surface and stress, can lead to a sharp increase of the frequency of microseismic events. Normally, the cohesion of intact rock is in the range 1 MPa–100 MPa, and fractured rock asymptotes to 0. According to the Mohr-Coulomb criterion (Fig. 3.), the envelope for primary fractures (blue line) without rock cohesion approaches the limiting Mohr stress state than that of the solid intact rock (red line) (Fig. 3). Therefore, microseismic events will occur preferably on primary fractures rather than through solid intact rock.

Passive microseismic monitoring associated with stress changes in and around the reservoir can also be used to probe the reservoir dynamics in response to external and internal perturbations. A microseismic event analysis can be used to locate the fracturing, and to determine the orientation, height, length, complexity, and temporal growth of the induced fracture by using the recovered focal mechanism (Maxwell and Urbancic, 2001; Maxwell, 2010).

The focal mechanism of an earthquake describes the deformation in the source region that generates the seismic waves. In the case of a fault-related event, it refers to the orientation of the fault plane that slips with the slip vector also known as a fault-plane solution. The focal mechanism is derived from a solution of the moment tensor for the earthquake, which is estimated by an analysis of observed seismic waveforms.

The same seismic signals recorded on seismometers at different locations have similar amplitude-frequency characteristics. The seismic moment tensor is a mathematical description of the deformation mechanisms in the immediate vicinity of the seismic source. It characterizes the seismic event magnitude, the failure mode and the fracture orientation. The seismic moment tensor is a second-order tensor with nine components, defined by a 3 × 3 matrix as follows:

$$M = M_0 \begin{bmatrix} M_{11} & M_{12} & M_{13} \\ M_{21} & M_{22} & M_{23} \\ M_{31} & M_{32} & M_{33} \end{bmatrix} \quad (3)$$

where M_0 is the seismic moment and the M_{ij} components represent force couples composed of opposing unit forces pointing in the i-direction, separated by an infinitesimal distance in the j-direction. For the conservation of angular momentum, the condition $M_{ij} = M_{ji}$ must be satisfied, so the moment tensor is symmetric with just six independent components (Agharazi, 2016).

When determining the arrival-time shifts, the selected data has waveforms clearly defining a standard track. Then a cross-correlation is made between other waveforms and the standard waveform to obtain the position of the correlation coefficient with the largest absolute value, so that the arrival-time shifts can be obtained.

Aligning all tracks in time according to the arrival-time shifts, the recorded waveforms are then added to the to the standard waveform. If the waveform amplitude of the standard track increases, it is possible to then define whether the initial motion direction of record track and the standard track is consistent, otherwise, the initial motion direction of the two is considered inconsistent. The initial motion direction of the microseismic events can be determined one by one based on this method. In general, in front of the crack, if the amplitude of initial motion is upward, the signal is labeled positive, and behind the crack, if the initial motion amplitude is downward, it is labeled as negative. Combined with the array of monitoring stations, the initial sign distribution of all microseismic events can be described on a plane.

The projection of all monitoring signals of a seismic source can be divided into four quadrants separated by two planes intersecting perpendicular to each other. The sense of compressional or dilative regions of the first arrivals are equivalent in spaces that are diagonally adjacent. Where the signs in diagonal spaces are identical, and in adjacent spaces are opposite, then the microseismic event is judged to be a strike slip fracture and the orientation of the nodal plane is the fracture trend. If the projection of all monitoring signals of the seismic source can be divided into two spaces by a straight line, and the signs in adjacent spaces are opposite then the microseismic event is judged to be a dip slip fracture, and the cutoff line is consistent with the crack trend. If the projection of all monitoring signals of the seismic source can be divided into two spaces by a closed ellipse, and the initial sign of the inside and outside of the ellipse is inconsistent, then the microseismic event is judged to be a tensile fracture, and the direction of the long axis of the ellipse indicates the crack trend (Liu, 2013).

3.2. Microseismic monitoring

Microseismic monitoring within this study was performed by using an OMNI2400 system manufactured by Geospace Technologies (USA) with a sensitivity of 52 VS/m and stationary frequency from 15 Hz to 1500 Hz. The sampling frequency is 1000 Hz and the lower limit of earthquakes monitoring is magnitude −3.

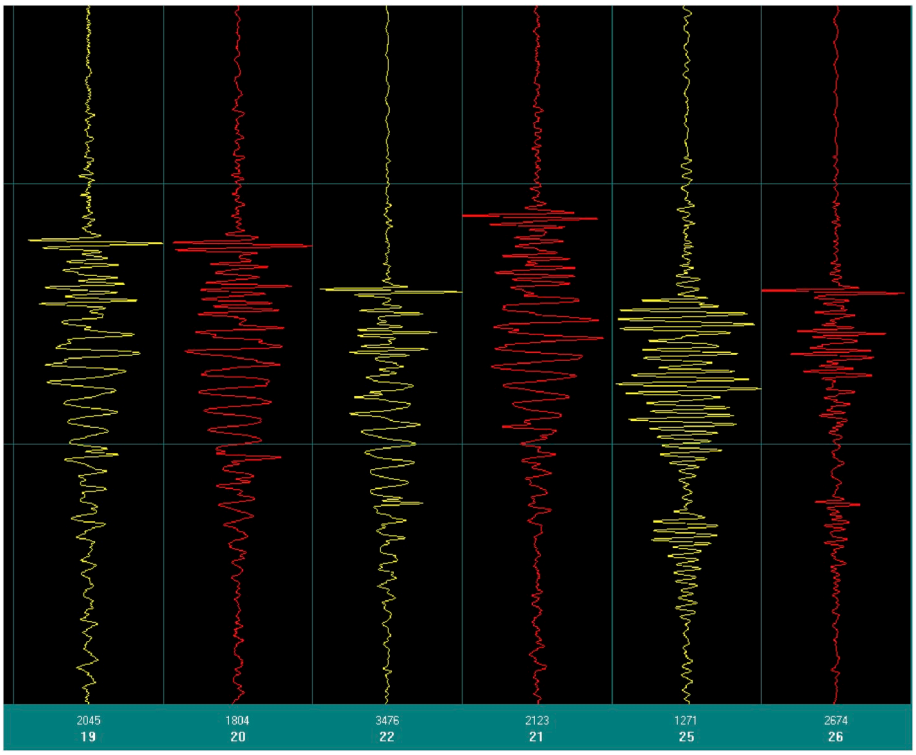

Fig. 4. Typical microseismic waveforms. (The vertical axis of diagram represents the travelling-time that was used for locating microseismic events. The first number (2045, 1804 …) beneath the diagram is the peak voltage amplitude, and the second row (19, 20, 22 …) is the monitoring station code.**).**

Table 2
Microseismic event counts for all monitoring wells.

Well ID	Number of micro seismic events	Number of tensile events	Number of dip slip events	Number of strike slip events
HG78	68	9	20	39
HG79	62	5	16	41
HG82	63	9	14	40
HG83	61	4	21	36
HG85	48	5	16	27
HG86	60	8	22	30
HG87	34	4	10	20
HG88	54	11	11	32
HG95	43	7	12	24
HG173	47	3	15	29

Event monitoring was applied to ten CBM wells in the study area between December 2017 and January 2018. According to the well spacing, the monitoring stations were distributed in a star-like pattern over a spatial range of 100 m–150 m (Fig. 2) from the wellhead. In order to ensure parallel comparison amongst the monitoring data, the monitoring time for each well was set to be 2 h.

4. Results and discussion

4.1. Microseismic event structure

A total of 870 distinct microseismic events were recorded from the 10 investigated wells. The waveforms are clear, and the seismic arrival time can be accurately distinguished (Fig. 4). A detailed velocity model with ten layers was constructed from sonic logs of the well, and the arrival time of each point 5 m apart was calculated. This allowed correction to the seismic events of different phases and ray path orientations to “matches”. Then a database of event locations was prepared for fracture imaging. All of these data were analyzed using inhouse software based on the methodology described in Section 3.1, specially developed for CBM well microseismic event analysis.

The 10 CBM wells in the study area were arranged in a diamond shape spaced about 250 m apart – resulting in a mean radius of influence of each well of about 125 m. In order to describe the primary reservoir fractures present in each well, full waveform microseismic events within the radius of 125 m were collected as listed in Table 2. These microseismic events are unevenly distributed with the number of events decreasing from a maximum of 68 (well #HG78) to a minimum of 34 (well #HG87), with an average of 54 for all wells.

4.2. Focal mechanisms

Focal mechanism analysis has been extensively used for the characterization of subsurface formations to evaluate geomechanical behavior during hydraulic injections, notably in the geothermal industry (Pearson, 1981; Jupeet et al., 1992; Feng and Lees, 1998; Sasaki, 1998). Most recently, applications in the petroleum industry have focused on hydro-fracture mapping and interpretation, combined with advanced applications in microseismic moment tensor and focal mechanisms analysis (Nolen-Hoeksema and Ruff, 2001; Rutledge et al., 2004; Baig and Urbancic, 2010). Studies of natural fractures in cores of Barnett Shale concluded that preferential reactivation of the pre-existing fracture network could affect hydro-fracture stimulations by re-directing fluid flow (Gale et al., 2007). Therefore, microseismic focal mechanisms have the potential to characterize and quantify reservoir permeability.

The various microseismic events into tensile, dip slip and strike slip events were distinguished through analysis of the focal mechanisms. The distribution of different types of fractures for each well is listed in Table 2 and plotted in Fig. 5. Strike slip events are the most frequently occurring, followed by dip slip events with tensile events the least frequent. Tensile fractures were monitored and well represented in five wells including HG88 (11), HG82 (9), HG78 (9), HG86 (8) and HG95 (7), with the spatial distribution of these five wells along the NE

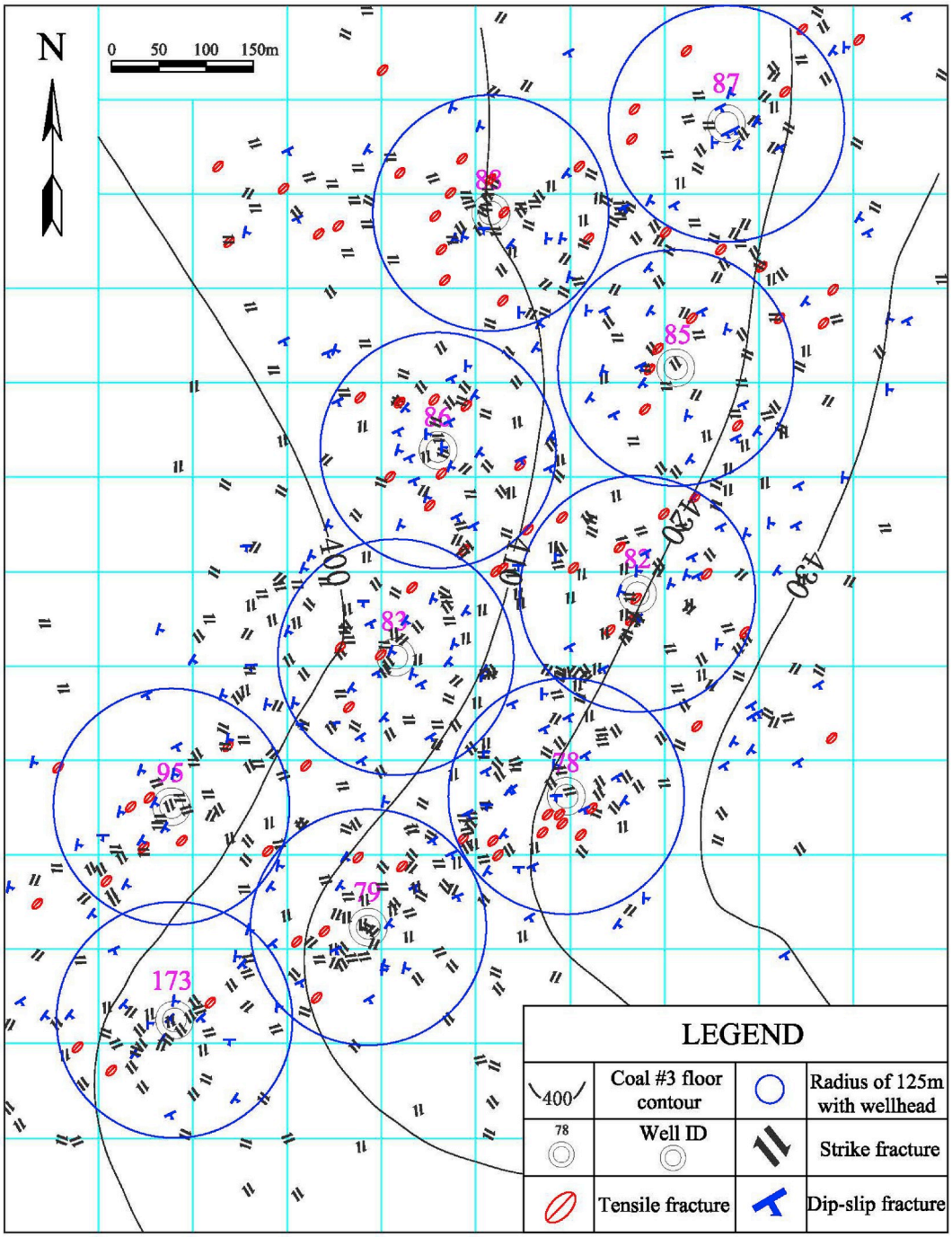

Fig. 5. Distribution of primary fractures by focal mechanism.

direction.

It is widely accepted that the permeability of subsurface fractures and faults directly relates to in situ stress magnitude and stress heterogeneity. Some fractured gas reservoirs show that fracture-controlled well performance is significantly impacted by stress fields perturbed by faults (Tamagawa and Pollard, 2008). Recent seismic movement along fractures (faults) might change the local stress state at the scale of oil field structures in southern California (Castillo and Zoback, 1994). Active deformation related to fault movement generates fractures and results in local stress-field perturbations, each of which affect permeability in the vicinity of the faults. Based on these findings, the authors propose that the contribution of fractures to reservoir permeability is, in approximate order, tensile > dip slip > strike slip cleats (Fang et al., 2018; Li et al., 2019; Hennings et al., 2012; Busetti and Reches, 2014; Eyre and van der Baan, 2015; Williams et al., 2012; Zhao et al., 2019). In terms of the frequency and geomechanical properties of primary fractures in the studied area, it is inferred that the permeability follows the following order from high to low, HG82, HG78, HG79, HG83, HG86, HG88, HG85, HG173, HG95 and HG87.

4.3. Correlations against gas production in CBM wells

The permeability adjacent to the CBM wells in the study area is generally ultralow and contributes to a very low overall gas flow. Commercially viable gas flows cannot be economical unless the formation can be effectively stimulated with extensive induced fracture

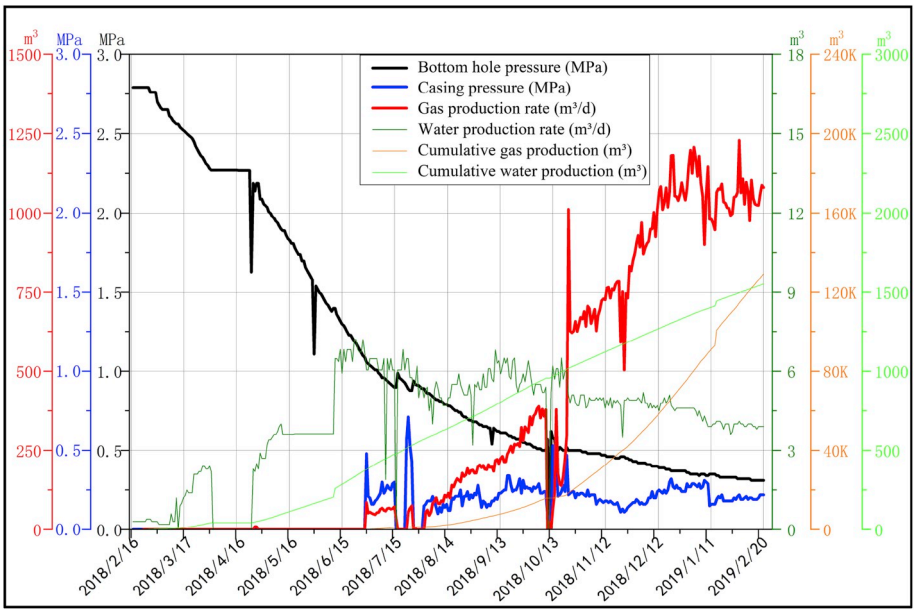

Fig. 6. Production data for well HG83.

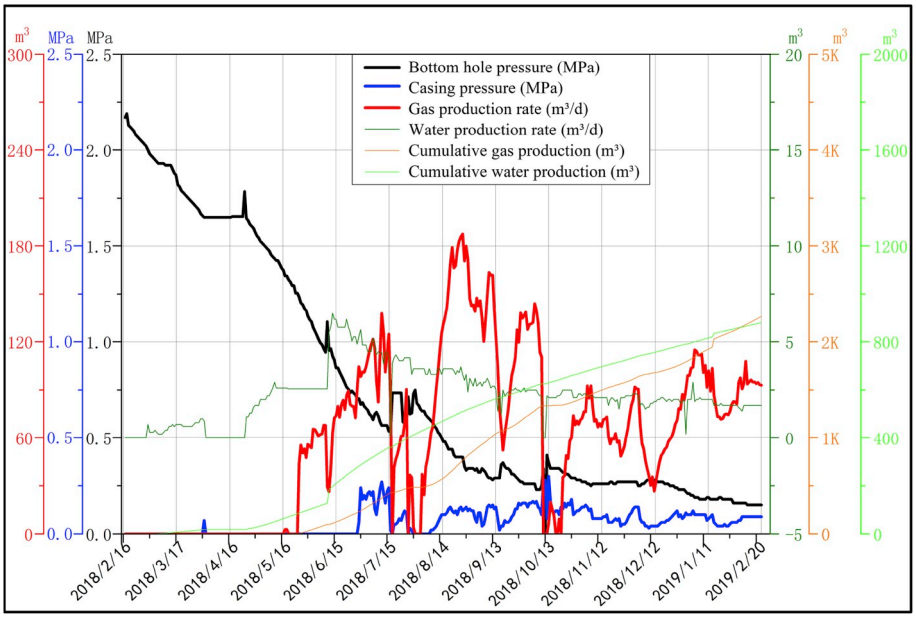

Fig. 7. Production data for well HG87.

Table 3
Gas production data for the 10 wells.

Well ID	Maximum (m^3/d)	Cumulative (m^3)	Well ID	Maximum (m^3/d)	Cumulative (m^3)
HG78	298.5	39807.4	HG86	821.8	105702.7
HG79	141.9	11052.2	HG87	187.7	22628.3
HG82	535	83402.1	HG88	373.1	16635.9
HG83	1228.8	129364.2	HG95	284.3	29159.2
HG85	945	59911.1	HG173	483.2	43481.6

Where: Maximum is the maximum gas production of each coalbed methane well; Cumulative production is the total gas production within the first 14 months.

networks. When the formation is effectively stimulated, the complex and well-connected fracture network will provide the gas pathways for gas production (Walton and McLennan, 2013).

The 10 CBM wells within the study area were hydraulically stimulated in December 2017, followed by dewatering and gas production for about 14 months. The maximum daily gas production is 1228.8 m^3/d in well HG83, followed by 945 m^3/d in HG85 and 821.8 m^3/d in HG86. For the low production wells, HG79 and HG87 can only produce 141.9 m^3/d and 187.7 m^3/d, respectively. In terms of cumulative gas production, HG83 and HG86 produced more than 100,000 m^3during the first 14 months, followed by HG82 (83402.1 m^3) and HG85 (59911.1 m^3). Typical production profiles are shown in Figs. 6 and 7 with detailed production data for all wells collected and detailed in Table 3.

The recorded gas production data and the cumulative number of microseismic events are plotted together in Fig. 8. As a general trend, the higher the number of microseismic events, the higher the gas production from the stimulated wells. However, there are outliers where the gas production is poor but with a relatively high number of microseismic

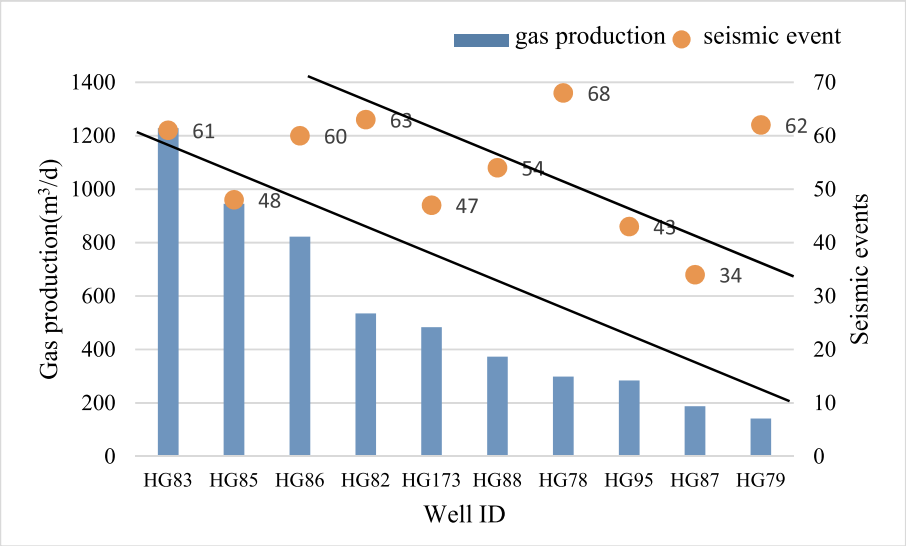

Fig. 8. Gas production by well number and cumulative number of seismic events within the tributary area of specific wells.

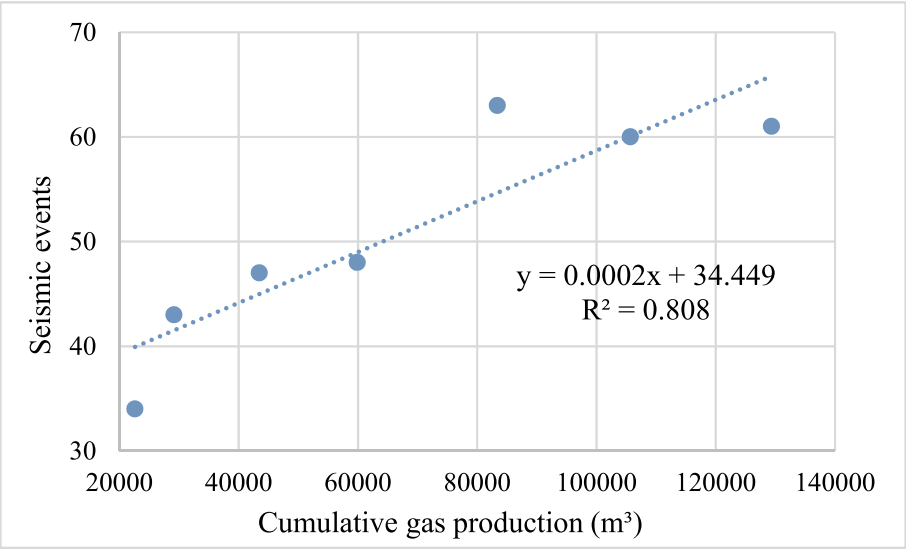

Fig. 9. Correlation between cumulative gas production and the cumulative number of microseismic events.

events, e.g. for wells HG78, HG79 and HG85.

After removing the three outliers, we make a correlation between the cumulative gas production and microseismic events for the remaining 7 wells – with a correlation coefficient is 0.808 (Fig. 9). In other words, in a reasonable degree of confidence, there is a significant correlation between CBM well production and cumulative number of microseismic events. This result was also verified by Grechka et al. (2010) who pointed out that gas rates can be predicted from microseismic with a tight gas study in Pinedale, Wyoming, USA.

These results indicate that the frequency of microseismic events obtained from passive microseismic monitoring can be used as a proxy to evaluate the fracturing system and transport properties of the coal seam and estimate gas production potential. As shown in Tables 2 and 3 and Fig. 8, more microseismic events or fractures were monitored from the two wells HG78 and HG79 that should have high production, but they produced relatively less, either in daily rate or accumulatively. Thus the uncertainties suggest that: (1) the microseismic events correlate directly with the generation of the fracture network, but may not directly correlate with the fracturing-induced change in permeability of the formation, (2) the microseismic events correlate with the fracture network and also directly correlate with the increase in permeability of the formation for the seven most productive wells, but that permeability does not always correlative with gas production due to other mitigating factors such as low initial gas content or other geological conditions. It is our understanding that (2) is a more reliable possibility: a formation with higher permeability is not always productive since other unknown factors may exist around the well, which occurs frequently in CBM blocks where geological structures are complex. In this area, may an undetected small karst collapse columns existing between the wells can induce the coal gas content low then production low. Other than geological causes, engineering problems, such as hydraulic fracturing and pumping control (Meng et al., 2011), also lead to low gas rates. Thus, further studies will be required to transfer the microseismic events to the permeability and production, and geologic condition.

In summary, the microseismic event survey is a feasible technique to predict the gas potential of a CBM reservoir through the number of passive microseismic events, and it has been confirmed at the studied area. Thus, it is concluded that passive microseismic survey is a new technology to characterize coal reservoir permeable properties, and further evaluate CBM production potential.

5. Summary and conclusions

In this study, microseismic monitoring and recording was conducted for ten CBM wells covering an overall area of 1.2 km^2 at one active CBM production basin in China. The results provide an understanding of the primary fracture system in the coal bearing formation. The geomechanical attribution of the fractures were quantitatively investigated through a focal mechanism. Based on the theoretical and field investigation results, the following conclusions can be made.

(1) The fracture characteristics of the coal formation including fracture density and geomechanics can be monitored and recorded using a microseismic monitoring technique. The results are consistent with the outcrop field measurements, which indirectly proves that passive microseismic monitoring is a new technology for fracture system characterization for CBM formations.
(2) A total of 870 effective microseismic events were detected and recorded in this study. We found that the microseismic events are unevenly distributed in the studied area.
(3) The geomechanical properties of all of the seismic events were analyzed with focal mechanism methodology. The results show that the primary fractures in the studied area are mainly strike slip type followed by dip slip, and that the tensional type is the least prevalent.
(4) Gas production generally correlates with microseismic events with a few exceptions which demonstrate that the technique can be used for CBM reservoir evaluation.

CRediT authorship contribution statement

Lin Tian: Methodology, Investigation, Writing - original draft. **Yunxing Cao:** Conceptualization, Methodology. **Shimin Liu:** Writing - review & editing. **Bin Shi:** Data curation. **Jianzhong Liu:** Methodology, Software. **Derek Elsworth:** Writing - review & editing.

Acknowledgments

This research was funded by the National Major Research Program for Sciences and Technology of China (Grant Nos. 2016ZX05067006-002 and 2017ZX05064002) and the National Natural Science Foundation of China (No.41372159). We especially thank the various operators for supplying micro-seismic data and for enabling this work. We also thank Chaoyu Tang for assistance in interpreting the micro-seismic results.

Appendix A. Supplementary data

Supplementary data to this article can be found online at https://doi.org/10.1016/j.jngse.2020.103181.

References

Agharazi, A., 2016. Determining maximum horizontal stress with microseismic focal mechanisms- Case studies in the Marcellus, Eagle Ford, Wolfcamp. In: UREeC: 2461621 Presented at the Unconventional Resources Technology Conference, San Antonio, Texas, USA, 1-3 August.
Baig, A., Urbancic, T., 2010. Microseismic moment tensors: a path to understanding frac growth. Lead. Edge 29 (3), 320–324.
Bo, D.M., Zhao, Y.J., Jiang, L., Gong, Y.J., Li, Z.L., 2008. Progress of the research on coalbed gas reservoir permeability. J. Southwest Petrol. Univ. 30 (6), 31–34 (in Chinese).
Busetti, S., Reches, Z., 2014. Geomechanics of hydraulic fracturing microseismicity: Part 2. Stress state determination. AAPG Bull. 98 (11), 2459–2476.
Cai, Y.D., Liu, D.M., Yao, Y.B., Li, J.Q., Qiu, Y.K., 2011. Geological controls on prediction of coalbed methane of No.3 coal seam in Southern Qinshui Basin, North China. Int. J. Coal Geol. 88, 101–112.
Cao, Y., Long, S.X., Li, X.Z., 2014. The enlightenment from comparative studies of the coalbed methane development at home and abroad. J. Xinjiang Petrol. Geol. 35 (1), 109–113 (in Chinese).
Castillo, D.A., Zoback, M.D., 1994. Systematic variations in stress state in the southern San Joaquin Valley. AAPG Bull. 78, 1257–1275.
Chen, S.D., Tang, D.Z., Tao, S., Xu, Hao, Zhao, J.L., Fu, H.J., Ren, P.F., 2018. In-situ stress, stress-dependent permeability, pore pressure and gas-bearing system in multiple coal seams in the Panguan area, western Guizhou, China. J. Nat. Gas Sci. Eng. 49, 110–122.
Combs, J., Hadley, D., 1977. Microearthquake investigation of the Mesa geothermal anomaly, Imperial valley, California. Geophysics 42 (1), 17–33.
Davis, G.H., Reynolds, S.J., Kluth, C.F., 2011. Structural Geology of Rocks and Regions. John Wiley & Sons Inc, New York, 2011.
Detring, J.P., Williams-Stroud, S., 2012. Using microseismicity to understand subsurface fracture systems and increase the effectiveness of completions: Eagle Ford Shale, TX. In: Paper SPE 162845 Presented at the SPE Canadian Unconventional Resources Conference, vol. 30 (Calgary, Alberta, Canada).
Dixon, J.M., 1979. Techniques and Tests for Measuring Joint Intensity (PhD Thesis). West Virginia University.
ECE ENERGY SERIES, 2010. Best Practice Guidance for Effective Methane Drainage and Use in Coal Mines (New York and Geneva).
Eyre, T.S., van der Baan, M., 2015. Overview of moment-tensor inversion of microseismic events. Lead. Edge 34, 882–888.
Fang, Y., Elsworth, D., Cladouhos, T.T., 2018. Reservoir permeability mapping using microearthquake data. Geothermics 72, 83–100.
Feng, Q., Lees, J.M., 1998. Microseismicity, stress, and fracture in the Coso geothermal field, California. Tectonophysics 289, 221–238.
Gale, J.F.W., Reed, R.M., Holder, J., 2007. Natural fractures in the Barnett Shale and their important for hydraulic fracture treatments. AAPG Bull. 91 (4), 603–622.
Grechka, V., Mazumdar, P., Shapiro, S.A., 2010. Predicting permeability and gas production of hydraulically fractured tight sands from microseismic data. Geophysics 75, B1–B10.
Groshong Jr., R.H., Pashin, J.C., McIntyre, M.R., 2009. Structural controls on fractured coal reservoirs in the southern Appalachian Black Warrior foreland basin. J. Struct. Geol. 31 (9), 874–886.
Hennings, P., Allwardt, P., Paul, P., Zahm, C., Reid Jr., R., Alley, H., Kirschner, R., Lee, B., Hough, E., 2012. Relationship between fractures, fault zones, stress, and reservoir productivity in the Suban gas field, Sumatra, Indonesia. AAPG Bull. 96 (4), 753–772.
Jupe, A., Cowles, J., Jones, R., 1998. Microseismic monitoring: listen and see the reservoir. World Oil 174, 171–172.
Jupeet, A.J., Green, A.S.P., Wallroth, T., 1992. Induced microseismicity and reservoir growth at the Fallback hot dry rocks project, Sweden. Int. J. Rock Mech. Min. Sci. Geomech. Abstr. 29 (4), 343–354.
Lacazette, A., Laudon, C., 2015. Ambient seismic imaging throughout the unconventional field's life cycle. J. Petrol. Technol. 67, 32–35.
Laubach, S.E., Marrett, R.A., Olson, J.E., et al., 1998. Characteristics and origins of coal cleat: a review. Int. J. Coal Geol. 35, 175–207.
Li, L., Tan, J.Q., David, A.W., Zhao, Z.G., Becker, D., Qiao, L., Shu, B., Chen, H.C., 2019. A review of the current status of induced seismicity monitoring for hydraulic fracturing in unconventional tight oil and gas reservoirs. Fuel 242, 195–210.
Liao, Y.Y., Luo, D.K., Li, W.D., 2012. Development strategy analysis of China's CBM. Acta Petrol. Sin. 33 (6), 1098–1102 (in Chinese).
Liu, J.Z., 2013. A Method of Focal Mechanism Analysis Using Microseismic Events. China, Patent CN103076634 A. 2013.05. (in Chinese).
Malin, P.E., Blakeslee, S.N., Alvarez, M.G., Martin, A.J., 1989. Microearthquake imaging of the Parkfield asperity. Science 244, 557–559.
Maxwell, S., Urbancic, T.I., 2001. The role of passive microseismic monitoring in the instrumented oil field. Lead. Edge 20, 636–640.
Maxwell, S., 2010. Microseismic: growth born from success. Lead. Edge 29 (3), 338–343.
Maxwell, S., Rutledge, J., Jones, R., Fehler, M., 2010. Petroleum reservoir characterization using downhole microseismic monitoring. Geophysics 75A, 129–137.
Men, X.Y., Han, Z., Gao, B.S., Ren, J.H., Cui, B.L., 2017. Present situation and development suggestion of CBM exploration and development in China. J. China Min. 26 (S2), 1–4 (in Chinese).
Men, X.Y., Han, Z., Gong, H.J., Wang, Y.Y., 2018. Challenges and opportunities of CBM exploration and development in China under new situations. Nat. Gas. Ind. 38 (9), 10–15 (in Chinese).
Meng, Z.P., Zhang, J.C., Wang, R., 2011. In-situ stress, pore pressure and stress-dependent permeability in the Southern Qinshui Basin. Int. J. Rock Mech. Min. Sci. 48, 122–131.
Mu, F.Y., 2017. CBM Industry Progress in China. petroleum industry press, Beijing, 2017. (in Chinese).
National energy administration, 2005. General Scheme of Coal Mine Gas Control and Utilization. National development and reform commission of China, 2005.
National energy board, 2007. Overview and Economics of Horseshoe Canyon Coalbed Methane Development. Canada, 2007.
Nolen-Hoeksema, R.C., Ruff, L.J., 2001. Moment tensor inversion of microseismic from the B-sand propped hydro-fracture, M-site, Colorado. Tectonophysics 336, 163–181.
Palmer, I., 2010. Coalbed methane completions: a world view. Int. J. Coal Geol. 82, 184–195.
Pashin, J.C., Groshong Jr., R.H., 1998. Structural control of coalbed methane production in Alabama. Int. J. Coal Geol. 38, 89–113.
Pearson, C., 1981. The relationship between microseismicity and high pore pressures during hydraulic stimulation experiments in low permeability granitic rocks. J. Geophys. Res. 86 (9), 7855–7864.
Research center of oil & gas resource strategies, 2009. Ministry of Land and Resources. National Coalbed Methane Resources Evaluation. China Land Press, Beijing, p. 256.

Rodvelt, G., Oestreich, R., 2008. Best practices for obtaining quality permeability data with CBM matrix injection-falloff testing. In: Paper 0827 Presented at the International Coalbed and Shale Gas Symposium. Tuscaloosa, Alabama, USA.

Rutledge, J.T., Phillips, W.S., Mayerhofer, M.J., 2004. Faulting induced by forced fluid injection and fluid flow forced by faulting: an interpretation of hydraulic-fracture microseismicity, Carthage Cotton Valley gas field. Texas. Bull. Seism. Soc. Amer. 94, 1817–1830.

Sasaki, S., 1998. Characteristics of microseismic events during hydraulic fracturing experiments at the Hijori hot dry rock geothermal energy site, Yamagata, Japan. Tectonophysics 289, 171–188.

Tamagawa, T., Pollard, D.D., 2008. Fracture permeability created by perturbed stress fields around active faults in a fractured basement reservoir. AAPG Bull. 92, 743–764.

Tian, L., Cao, Y.X., Chai, X.Z., Liu, T.J., Feng, P.W., Feng, H.M., Zhou, D., Shi, B., Oestreich, R., Rodvelt, G., 2015. Best practices for the determination of low-pressure/permeability coalbed methane reservoirs, Yuwu coal mine, Luan mining area, China. Fuel 160, 100–107.

Walton, I., McLennan, J., 2013. The role of natural fractures in shale gas production. In: International Conference for Effective and Sustainable Hydraulic Fracturing, Brisbane, Australia, 20-22 May. https://doi.org/10.5772/56404.

Wheeler, R.L., Dixon, J.M., 1980. Intensity of systematic joints: methods and application. Geology 8, 230–233.

Williams, S.C., Barker, W.B., Smith, K.L., 2012. Induced hydraulic fractures or reactivated natural fractures? Modeling the response of natural fracture networks to stimulation treatments. In: 46th US Rock Mechanics/Geomechanics Symposium, Chicago, June 24-27. American Rock Mechanics Association.

Yu, D.B., 2007. Research on the cause analysis and prevent control on frequent heavy disaster in coal mine in China. Min. Saf. Environ. Protect. 34 (2), 76–79 (in Chinese).

Zhang, Z., 2016. Research and Application of the Corresponding Relationships between the Fractures in the Surrounding Rocks and Coal Reservoirs: a Case from Kubai Mining Area (PhD Thesis). China University of Geosciences.

Zhao, Y., Yang, T.H., Zhang, P.H., Xu, H.Y., Zhou, J.R., Yu, Q.L., 2019. Method for generating a discrete fracture network from microseismic data and its application in analyzing the permeability of rock masses: a case study. Rock Mech. Rock Eng. 52, 3133–3155.